IOP FTC
IOP PUBLISHING JOURNAL OF PHYSICS B: ATOMIC, MOLECULAR AND OPTICAL PHYSICS
J. Phys. B: At. Mol. Opt. Phys. **41** (2008) 021001 (4pp) doi:10.1088/0953-4075/41/2/021001

FAST TRACK COMMUNICATION

Study of low-energy resonant metastability exchange in argon by a pulsed merging beam technique

J Grucker[1], J Baudon[1], F Perales[1], G Dutier[1], G Vassilev[1], V Bocvarski[2] and M Ducloy[1]

[1] Laboratoire de Physique des Lasers (UMR-CNRS 7538), Université Paris 13, Av. J.B. Clément, 93430-Villetaneuse, France
[2] Institute of Physics, Belgrade, Pregrevica 118, 11080, Zemun, Serbia

E-mail: grucker@galilee.univ-paris13.fr

Received 14 November 2007, in final form 16 November 2007
Published 8 January 2008
Online at stacks.iop.org/JPhysB/41/021001

Abstract
The resonant metastability exchange process in low-energy collinear collisions between metastable argon atoms (Ar* $^3P_2$) polarized in spin ($M = +2$) and ground-state Ar atoms from a nozzle beam is studied by means of a time-of-flight technique. A wide range of metastable atom velocities in the laboratory frame (275 m s^{-1} down to 50 m s^{-1}) is obtained by use of a Zeeman slower, the counter-propagating laser beam of which is locked in frequency onto the $^3P_2$–$^3D_3$ closed transition ($\lambda = 811.5$ nm). The accessible centre-of-mass energy range (8–27 meV) has not been explored so far, to our knowledge. Calculations based upon existing interatomic potentials of 2_g and 2_u symmetries are in reasonable agreement with experiment.

Merging beams have proven to be a very efficient tool to measure charge-exchange total cross sections in ion–atom and atom–atom [1, 2] collisions at low and very low energies. The basic idea is to use two superimposed beams within which particles move at high but close velocities. Hence the relative velocity is low and the collision energy is small, and actually much smaller than the energy difference between the two species. For example, energies $E_1 = 3$ keV and $E_2 = 3.1$ keV in the laboratory reference frame lead to a collision energy in the centre-of-mass (cm) frame $E_c = 0.42$ eV. Such experiments are characterized by a high accuracy in the energy definition (10^{-4} or less), a well-defined beam geometry and a good knowledge of the detection efficiencies. Nevertheless some difficulties remain to get an absolute value of the total cross section: (i) the overlap of the beam profiles is not precisely known and even suspected to vary during the measurement, (ii) one has to discriminate few beam–beam collisions from numerous beam-(background) gas collisions. The first difficulty can be overcome by sweeping transversally one beam over the other one [2], the second difficulty by applying an electrostatic potential to a specific portion of the beams. Whilst it is based upon the same principles, the present experiment differs from the previous ones by many aspects. The two species involved here are ground-state and metastable argon atoms and the process under consideration is the resonant metastability exchange, namely Ar*($^3P_2$) + Ar → Ar + Ar*($^3P_2$). Both species initially move at the same thermal velocity ($v_0 = 560$ m s^{-1}, corresponding to a kinetic energy of 65 meV). Metastable atoms are then slowed down by use of a Zeeman slower providing final velocities v_f in the range 275–50 m s^{-1}, i.e. a kinetic energy in the range 15.7 meV–0.52 meV. As a consequence the 'kinematical contraction' mentioned above no longer holds since the collision energy E_c in the centre-of-mass frame ranges from 8 to 27 meV. Actually this experiment is interesting for several reasons. (i) The resonant metastability exchange at low energy is a key process in the production of metastable atom beams of a high brightness and large coherence width [3]. Such beams are readily useable in various applications in coherent atom optics, such as atom interferometry, surface probing or nano-lithography. (ii) To our knowledge, no measurement of the exchange cross section in this energy range has been carried out so far. (iii) As

explained later, metastable atoms are spin-polarized (Zeeman state $M = +2$), which will greatly simplify the theoretical treatment of the collision. Another important difference with most of the previous merging beam experiments is the pulsed operating mode used in the present case.

Ground-state argon atoms are produced by a so-called 'high-enthalpy' Campargue- type generator [4], in other words a nozzle beam, the characteristics of which are as follows: a mean longitudinal velocity of 560 m s^{-1}, effective diameter of the nozzle 15 μm, relative velocity dispersion $\delta v/v = 1$–2%, angular aperture better than 0.4 mrad. 'Primary' metastable atoms (Ar* $^3P_0$, $^3P_2$) are produced by bombarding the nozzle beam with 100–150 eV electrons in a converging magnetic field. The recoil effect resulting from this bombardment significantly alters the genuine properties of the nozzle beam ($\delta v/v = 7$–8%, angular aperture of several mrad). Actually these properties are recovered owing to the resonant metastability exchange process, taking place between these 'primary' metastable atoms and the ground state atom nozzle beam. Indeed in this process the velocities of the two species are almost perfectly exchanged, which generates a 'secondary' metastable atom beam within which the velocity distribution, in modulus and angle, is identical to that of the nozzle beam. This effect has been observed for a while on He* (2^1S, 2^3S) metastable atoms by Brutschy and Haberland [5], by use of a time-of-flight technique. In their case the electrons move in the same direction as the atoms so that primary metastable atoms are slightly faster than the secondary ones. It is the contrary in our case. The contrast of the secondary metastable atom flux with respect to that of primary ones can be enhanced by use of a circular diaphragm (diameter 80 μm) located at 116 mm from the nozzle [3].

Metastable Ar* ($^3P_2$) atoms are slowed down using a so-called Zeeman slower, operating with a laser locked on the $^3P_2$–$^3D_3$ closed transition at $\lambda = 811.5$ nm. The circularly polarized (σ^+) laser beam counter propagates with respect to the atom beam. It is injected by a metallic mirror inclined at 45°, which serves also as a secondary emission electrode. It is followed by a channel electron multiplier which will be used as a detector in time-of-flight (TOF) measurements. Travelling atoms are maintained on resonance with the laser all along the slower by compensating the Doppler shift by the Zeeman effect in a special configuration of a longitudinal magnetic field $B(z)$. Under saturation conditions and assuming $v \ll c$, the radiative force is a constant (cf equation (90) in [6]). For a σ^+ polarization and a perfect following of the resonance condition, it takes the simple form

$$F \approx -(\hbar/2)\Gamma k_L, \tag{1}$$

where Γ is the width of the upper level and k_L is the optical wave number.

Therefore the acceleration $A = dv/dt = F/m$ where m is the atomic mass, is a negative constant and the ideal z-dependence of the velocity takes the form:

$$v(z) = [v(0)^2 - 2|A|z]^{1/2}. \tag{2}$$

Because of the resonance condition, $B(z)$ is linearly dependent on $v(z)$ which leads to:

$$B(z) = \frac{\hbar k_L}{g\mu_B}[v(0)^2 - 2|A|z]^{1/2} + C, \tag{3}$$

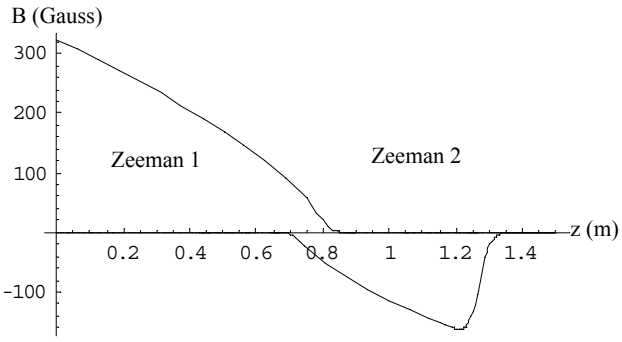

Figure 1. Longitudinal magnetic fields generated by the Zeeman coils (Zeeman 1 and Zeeman 2). Intensities are 300 mA and 150 mA, respectively.

where g is the Landé factor and μ_B is the Bohr magneton. The constant C is related to the chosen laser detuning Δ_L with respect to the atomic frequency. This form of $B(z)$ has been approached within the interval $0 \leqslant z \leqslant L_1$, L_1 being the length of this part Z_1 of the slower ($L_1 = 0.8$ m), by means of a proper ensemble of solenoidal current sheets of increasing radii and decreasing lengths. Actually, beyond $z = L_1$, these currents produce a monotonically decreasing field, which necessarily tends to zero at large distance. In order to get a well-defined non-zero final velocity v_f, this first part is followed by a second current system (Z_2) similar to the first one but shorter (length $L_2 = 0.3$ m) and reversed, generating a negative field with respect to the z axis (see figure 1). By an appropriate choice of Δ_L (here $\Delta_L = -340$ MHz) and $B(0)$ (here 300 G), one is able to 'tune' the slower on some nominal initial velocity $v(0)$ (here 600 m s^{-1}). At the end of Z_1 the velocity is about 275 m s^{-1}. Then, by adjusting the current in Z_2, one can choose the place where the total field abruptly changes its slope, i.e. the place where the atoms escape the slowing process, which defines the final velocity. Actually the motion is not exactly nominal since the initial velocity is 560 m s^{-1} instead of 600 m s^{-1}, but it can be shown that this has no consequence on the final velocity because of the strong longitudinal-velocity compression induced by the Zeeman slower.

As explained before slowed metastable atoms are observed by means of a TOF measurement over a distance of 1770 mm (±5 mm taking in account the secondary-emission plate inclination). A slotted disc is used to chop the beam. The chopping time (e.g., 16.8 μs at a motor frequency of 50 Hz) is smaller than the initial-beam TOF dispersion, 63 μs for $\delta v/v = 2\%$. Actually the disc chops both ground-state and metastable (detectable) atom (Ar* $^3P_2$ and $^3P_0$) beams, the only Ar* $^3P_2$ atoms being slowed down. At sufficiently low chopping period ($T < 200$ Hz), there is no chance that fast atoms overtake slow ones within the slower. Then an unperturbed TOF distribution of slow metastable atoms is observed. It is seen (figure 2) that for small enough final velocities this distribution is double peaked. This might be due to the geometry of atom and laser beams which do not perfectly match all along the slower.

At higher chopping frequency, fast ground state atoms (not slowed down) are allowed to overtake slowed-down metastable atoms issued from the preceding opening. Therefore

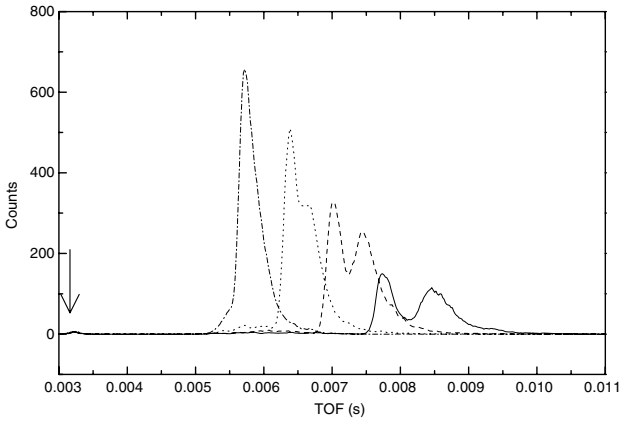

Figure 2. TOF spectra of slowed down metastable $Ar^*(^3P_2)$ atoms at various final velocities v_f: dash-dot line: 195 m s^{-1}, dotted line: 150–135 m s^{-1}, dashed line: 123–105 m s^{-1}, full line: 97–81 m s^{-1} (the two values correspond to the double peak structure). The TOF splitting increases as v_f decreases. The faster peak is narrower than the slower one. The relative widths $\delta t/t$ are respectively about 2–3% and 6–7%. The vertical arrow shows the initial TOF (v = 560 m s^{-1}).

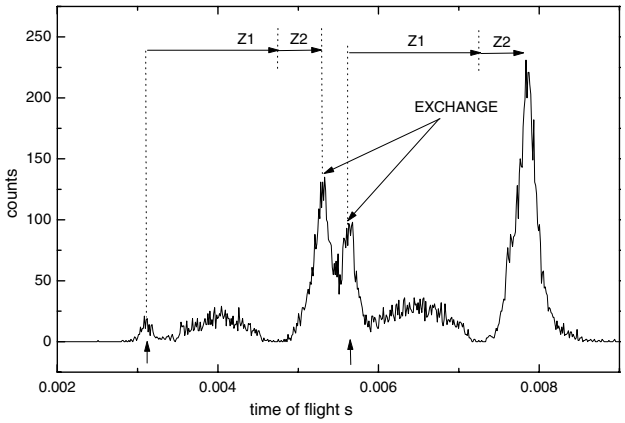

Figure 3. TOF spectrum obtained with the Zeeman slower $Z_1 + Z_2$ in operation (see text). The two vertical arrows indicate the TOFs of fast Ar* atoms issued from two slits separated in time by T = 2.5 ms. The slow atom peak of the 1st slit (TOF = 5.3 ms, v_f = 250 m s^{-1}) is reduced with respect to that of the 2nd slit (TOF = 7.8 ms), whereas the fast atom peak of the 2nd slit is enhanced by fast atoms generated by the exchange process. The present rather high final velocity (230 m s^{-1}) has been chosen for the sake of clarity of the spectrum. The wide peaks in between fast and slow contributions come from atoms imperfectly slowed down.

metastability exchange can occur within the slower itself. To study this process, one uses a slotted disc holding only two slits (width 1 mm, height 10 mm) placed at 90° from each other, on a radius of 95 mm. The first slit trigs the acquisition process. The motor frequency is set such that the time interval T between the openings of the two slits is smaller than the delay between the arrivals of fast and slowed atoms issued from the 1st slit. Under such conditions, the packet of fast ground-state atoms emitted by the 2nd slit overtakes the packet of slow metastable atoms issued from the 1st one. Fast metastable atoms produced by the exchange process reach the detector at the same time as fast metastable atoms (slower off) issued from the 2nd slit. The process does not repeat since the '3rd slit' is actually the 1st one, which is delayed by 3T with respect to the 2nd one. These features are clearly seen in the TOF spectrum shown in figure 3. This spectrum has been obtained with a motor frequency of 100 Hz (T = 2.5 ms). The two vertical arrows indicate the TOF-s of fast Ar* atoms coming from the 1st and 2nd slits. The peaks delayed by '$Z_1 + Z_2$' (horizontal arrows) correspond to metastable atoms slowed by Z_1 followed by Z_2 (final velocity v_f = 230 m s^{-1}). It is seen that the fast atom contribution of the 2nd slit (TOF of about 5.6 ms) appears much higher than that given by the 1st slit, whereas the slow atom contribution of the 1st slit is lower than that of the 2nd slit. This is due to the exchange process, which transforms the slow atoms of the 1st slit into fast ones, which appear just at the 'fast' TOF of the 2nd slit. From this excess of fast atoms, an exchange signal can be derived. Our goal here is not to analyse in detail the time dependence of the peaks but rather to get some information (from the integrals of the peaks) about the energy dependence of the exchange process. As a consequence the exact shape of the two overlapping packets and the way they exchange atoms can be ignored. Let v_0 = 560 m s^{-1} be the initial velocity. The initial relative velocity is then $v_r = v_0 - v_x$ where v_x is the slow atom velocity at the time of the overlap. To a very good accuracy, one has $v_x \approx v_f$. The corresponding centre-of-mass collision energy is $E_c = \frac{1}{2}\mu v_r^2$ where $\mu = m/2$ is the reduced mass. The explored final-velocity range is 50 m s^{-1}–275 m s^{-1}, the relative-velocity range is 285 m s^{-1}–480 m s^{-1}. The resulting centre-of-mass collision energy range is 7.8 meV $\leqslant Ec \leqslant$ 23.7 meV. Actually this range is limited towards low energies at about 10.5 meV because, for $v_f > 238$ ms^{-1} and T = 2.5 ms, the 2nd fast atom packet has no time enough to overtake the slow one before reaching the detector. As it is, this energy range has not been yet investigated experimentally, to our knowledge. Experimental points (in relative values) are shown in figure 4.

The scattering amplitude produced by one pair of molecular potentials of u- and g-symmetry related to the same value of Ω (absolute value of the projection on the internuclear axis **R** of the total internal angular momentum **J**) is given by [7] :

$$f(k,\theta_c) = f_g(k,\theta_c) + f_u(k,\theta_c) + f_g(k,\pi-\theta_c) - f_u(k,\pi-\theta_c), \quad (4)$$

where k is the atomic wave number in the centre-of-mass frame and $f_{g,u}$ are the amplitudes scattered by u, g potentials. The corresponding elastic differential cross section includes the so-called 'direct' scattering process (dominating around $\theta_c = 0$), the 'exchange' process (dominating around $\theta_c = \pi$) and their mutual interference. As we are only interested in the vicinity of $\theta_c = \pi$ we can ignore the additional nuclear-symmetry interference effect which mixes direct and exchange amplitudes and is dominant around $\theta_c = \pi/2$. At a large internuclear distance, **J** is simply the Ar* metastable atom internal momentum (J = 2). These atoms are initially polarised in the M = +2 magnetic sublevel and the **R** axis is along z. After the collision, in the vicinity of $\theta_c = \pi$, **R** is along

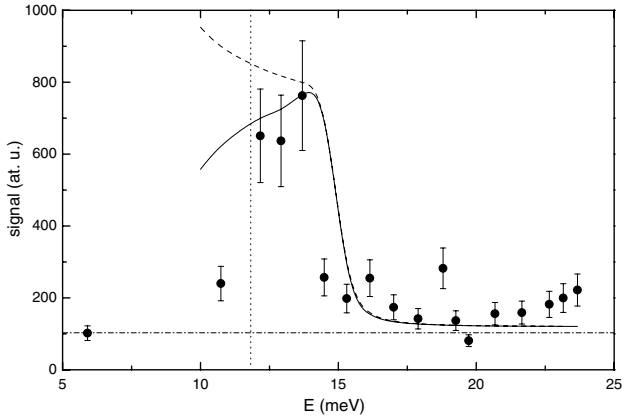

Figure 4. Exchange signal (see text) as a function of the centre-of-mass (cm) collision energy E_c. Points and error bars : experiment (arbitrary unit). The first experimental point at 5.8 meV corresponds to the background level (materialized by the horizontal dash-dotted line) since no exchange is observable at this energy. The vertical dotted line corresponds to the energy at which the exchange takes place at the detector position. Dashed line: calculated exchange signal using the differential cross section at cm scattering angle $\theta_c = \pi$. Full line: signal calculated by integrating over the energy-dependent cm angular acceptance of the detector. Calculated values are given in atomic unit.

$-z$. As exchanged atoms are also in the $M = +2$ state [8], the final molecular states have also the $\Omega = 2$ symmetry. The metastability exchange takes place mainly at large impact parameters, with almost no deflection. As a consequence rotational coupling effects leading to other Ω values are expected to be small. Finally it appears realistic to consider that only two potential symmetries are involved in the collision, namely 2_g, 2_u. Analytical molecular potentials $2_{g,u}$ of the Ar_2^* system have been proposed in the past [9] to interpret Ar* + Ar collision experiments at c.m energies ranging from 27.5 to 91 meV. These potentials are, in atomic units,

$$V_g(R) = -6.72\,10^4 R^{-6} + 6790\exp(-0.1187R)R^{-7.594}$$
$$V_u(R) = -6.72\,10^4 R^{-6} + 372.146\exp(-0.8162R)R^{-3.337}. \quad (5)$$

Even at collision energy as small as 10 meV, the JWKB approximation is still valid. From these potentials, JWKB phase shifts, $\delta_{g,u}(k, l)$, where l is the angular momentum of the relative motion, can be derived. Then the exchange amplitude is obtained from g, u-scattering amplitudes, which are given by the standard formula [10]

$$f_{g,u}(k, \theta_c) = (2ik)^{-1}\sum_{l=0}^{\infty}(2l+1) \times [\exp[2i\delta_{g,u}(k, l)] - 1]P_l(\cos\theta_c). \quad (6)$$

One finally gets the exchange differential cross section (DCS) $\sigma\ (k,\ \theta_c) = |f(k,\ \theta_c)|^2$. In figure 4 the signal derived from the differential cross section $\sigma(k, \pi)$ is plotted as a function of the cm collision energy E_c (dashed line). Actually our exchange signal is somewhat more intricate than this simple cm DCS. It corresponds to a DCS integrated over a limited, energy dependent, solid angle in the lab-frame. Geometrically this solid angle can be expressed as $\Delta\Omega_{lab} = 2\pi\left[1 - D_e\Big/\left(D_e^2 + S_d/\pi\right)^{1/2}\right]$ where $S_d \approx 200$ mm^2 is the detector area and D_e is the distance between the exchange place and the detector. Actually, in the present collinear configuration, the lab-frame solid angle is also limited because of the upper limit of the lab-scattering angle, namely $\theta_{max} = \arcsin[v_r/(v_r + v_f)]$. The corresponding value of the solid angle is then $\Delta\Omega'_{lab} = 2\pi(1 - \cos\theta_{max})$. The resulting signal is shown in figure 4. Its general behaviour is in agreement with experiment. Because of the contribution of angles close to π, it slightly oscillates around $\sigma(k, \pi)$, not as much however as the experimental data do. This might be due to a small defect in the potentials or, more likely, to a too crude estimate of the angular acceptance, which should be narrower than predicted. The present experiments have been carried out with the whole metastable atom beam, including both primary and secondary (i.e., exchanged) species. A significant improvement will be to isolate the secondary contribution, in which the velocity distribution is initially better defined than that of the primaries.

Note. The Interferometry and Optics with Atoms (IOA) group is a member of the Institut Francilien de Recherche sur les atomes froids (IFRAF).

References

[1] Peart B and Hayton D A 1994 *J. Phys. B: At. Mol. Opt. Phys.* **27** 2551–6
[2] Olamba K, Szücs S, Chenu J P, El Arbi Naji and Brouillard F 1996 *J. Phys.B : At. Mol. Opt. Phys.* **29** 2837
[3] Karam J-C, Wipf N, Grucker J, Perales F, Boustimi M, Vassilev G, Bocvarski V, Mainos C, Baudon J and Robert J 2005 *J. Phys. B : At. Mol. Opt. Phys.* **38** 2691
[4] Campargue R 1989 *J. Phys. Chem.* **88** 4466
[5] Brutschy B and Haberland H 1977 *J. Phys. E: Sci. Instrum.* **10** 90
[6] Lembessis V E, Babiker M, Baxter C and Loudon R 1993 *Phys. Rev.* A **48** 1594
[7] See: Aberth W, Lorents D C, Marchi R P and Smith F T 1965 *Phys. Rev. Lett.* **14** 776 This form of the exchange amplitude is exactly the same as that obtained for symmetric ion-atom charge exchange
[8] Perales F 1990 *PhD Thesis* Université Paris 13
[9] Robert J 1982 *Thèse de 3e Cycle* Université Paris Sud
[10] Landau L and Lifchitz E 1967 *Mécanique Quantique* (Moscow: MIR editions)